# A Simulation Approach to Determine Internal Architecture of 3D Bio-Printed Scaffold Suitable for A Perfusion Bioreactor Abstract ID: 2255

Scott Clark, Connor Quigley, Jack Mankowsky, MD Ahasan Habib\*

Sustainable Product Design and Architecture Department, Keene State College, Keene, NH 03435, USA.

#### Abstract

Traditional static cell culture methods don't guarantee access to medium inside areas or through the scaffolds because of the complex three-dimensional nature of the 3D bio-printed scaffolds. The bioreactor provides the necessary growth medium encapsulated and seeded cells in 3D bioprinted scaffolds. The constant flow of new growing medium could promote more viable and multiplying cells. Therefore, we created a specialized perfusion bioreactor that dynamically supplies the growth medium to the cells implanted or encapsulated in the scaffolds. A redesigned configuration of our developed bioreactor may enhance the in vivo stimuli and circumstances, ultimately improving the effectiveness of tissue regeneration. This study investigated how different scaffold pore shapes and porosities affect the flow. We employed a simulation technique to calculate fluid flow turbulence across several pore geometries, including uniform triangular, square, circular, and honeycomb. We constructed a scaffold with changing pore diameters to examine the fluid movement while maintaining constant porosity. The impact of fluid flow was then determined by simulating and mimicking the architecture of bone tissue. The best scaffold designs were chosen based on the findings.

## **Keywords**

3D bioprinting, Rheology, Shear Thinning, Printability.

## 1. Introduction

Creating complex patient-specific models using a variety of biomaterials encasing living cells in three dimensions (3D) is generally accepted [1]. This technique is creeping closer to accurately imitating tissue-specific microarchitecture as a growing tool for tissue engineering. Compared to laser and inkjet bioprinting, extrusion-based 3D bioprinting provides a superior deposit of various biomaterials with more cells encapsulated [2]. Natural hydrogels are good choices for bio-ink (biomaterial encasing living cells) because of their biocompatibility, minimal cytotoxicity, and high-water content (90%)[3]. However, only a few are normally employed to prepare bio-ink due to their poor mechanical strength and slow crosslinking rate [4]. The regeneration of injured tissue can be accelerated by effective cell-to-cell communication.[5]. The fundamental steps in tissue engineering are cell extraction, 2D culture incubation, cell proliferation, engineered scaffold construction, cell maturation in the scaffold (i.e., tissue formation), and application. Properly selecting a cell culture system, whether static or dynamic, is crucial. Traditional or static cell culture techniques suffer to offer the requisite nutrition for promoting cell proliferation and tissue development [6]. A bioreactor can be a critical tool to speed up cell proliferation because it can deliver growth medium on time [7, 8]. Particularly in perfusion bioreactors, new nutrients can flow dynamically and axially via scaffolds that have totally natural stimuli that influence cell growth and differentiation [7]. Recently, a perfusion bioreactor was created to test the bone scaffolds' mechanical characteristics and osteoblast responsiveness [9]. According to reports, a fully integrated organ bio-fabrication process has been demonstrated in a threefold perfusion bioreactor [10-12]. For the creation of designed aortic heart valves, a new pulsatile bioreactor design has been published [13, 14].

Tissue-engineering system modeling and simulation are useful to assess the impact of a 3D-scaffold architecture and associated bioreactor process parameters [9]. It is difficult to obtain internal information on the 3D-printed scaffold during incubation in the bioreactor because of the structure's inherent complexity. Hence, to examine the flow distribution and nutrient transport in complicated porous tissue scaffolds inside perfusion bioreactors, mathematical modeling and simulation techniques of the fluid dynamics in the tissue growing process are beneficial [15]. Various simulation approaches were utilized for the perfusion bioreactor to examine the fluid flow and its effects. A resolved scale numerical simulation was suggested to evaluate the overall culture condition, forecast cell growth rate, and define the supply of glucose inside a porous tissue scaffold in a perfusion bioreactor [16]. An efficient perfusion

system was created using computational fluid dynamics to replace the laborious trial-and-error experimental approach [17]. Using a COMSOL model, macroscale 3D printed vascular networks with different porosities were considered to forecast the oxygen transport gradient across the scaffold. Macroscale 3D printed vascular networks showed an increase in cell viability of up to 50% in experimental work [18]. Using computational analysis, fluid dynamics in 3D-printed scaffolds with various angular orientations between the strands in each layer were evaluated. However, the variational pore geometry was not analyzed in the work.

Recently, we created a unique perfusion bioreactor to dynamically deliver growth media to cells implanted or encapsulated in scaffolds [19]. The constant flow of new growing medium could promote more viable and multiplying cells. Perfusion bioreactors have been used in a range of tissue engineering applications due to their consistent nutrition delivery and flow-induced shear stress within the tissue-engineering scaffold. A redesigned configuration of our developed bioreactor may enhance the in vivo stimuli and circumstances, ultimately improving the effectiveness of tissue regeneration.

#### 2. Materials and Methods

## 2.1 Description of our designed and manufactured perfusion bioreactor

According to Figure 1, the bioreactor is comprised of five modules: the perfusion chambers, medium tanks, waste port, oxygen transfer, and perfusion pump. Many components around the bioreactor, including solenoid pinch valves, micro vacuums, and liquid level sensors, are controlled by the control unit with Arduino and a Breadboard. The Arduino is attached to a power source, a stepper driver, and a breadboard circuit that enables the conversion of lower signals into higher voltages. The microcontroller is attached to four output pins and one input pin. When tank 1 is full, the code executes a main loop for a predetermined period. After the main loop is finished, there is a waste loop that is performed to cycle away any unwanted cell waste. To ensure that medium cannot flow in an unauthorized manner, solenoid pinch valves are installed between tank two and tank one and between tank two and tank one. The valve connecting tank two and tank one is powered by 12V DC from the power source, and the pinch valves are generally closed. Although it operates at 24V DC from the power supply, the pinch valve between tank two and the waste tank is likewise generally closed. The power source, which also powers both Micro vacuums, provides 5V DC to the Arduino. The Bioreactor can operate in a closed loop thanks to this mechanism.

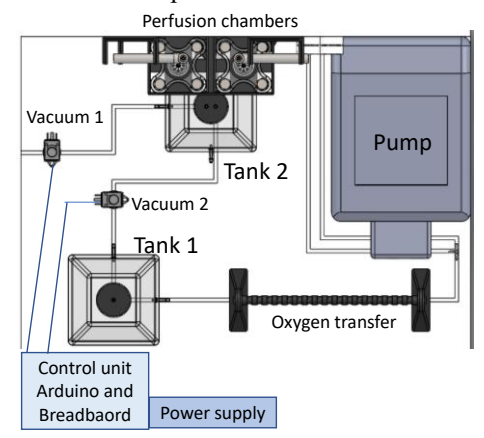


Figure 1: Modified design of bioreactor chamber compared to our previous design.

#### 2.2 Description Designing scaffold architecture.

A set of circular scaffolds (13 mm diameter) with various internal architectures, including honeycomb, triangular, random circular, and square, was created using a Computer Aided Design (CAD) program. These scaffolds are depicted in Figure 2. Every scaffold's pore size was the same. Between 66.4% and 72.5% of those scaffolds' porosity was considered. To study the effects of variational porosity on fluid flow during incubation in our bioreactor, we also created scaffolds with various pore sizes and geometries, as shown in Figure 2. (a-e). Depending on the sizes, geometries, and arrangement of the interior pores, the porosity ranged from 61.88% to 70.79%.

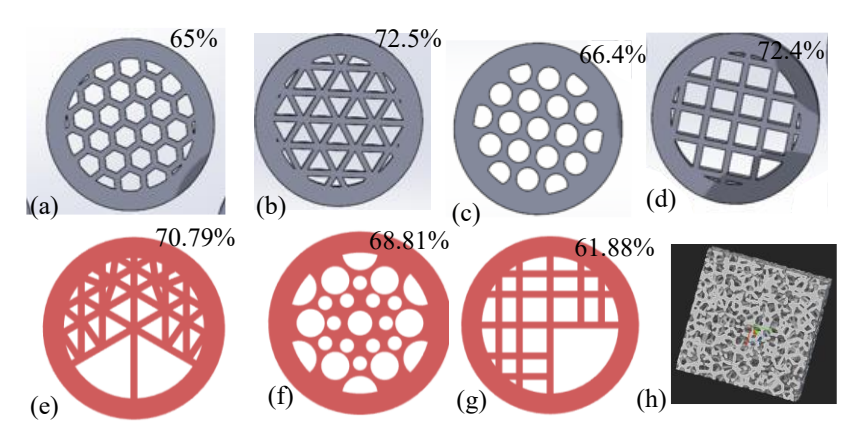


Figure 2: 3D models used for simulation having various internal architectures: (a) honeycomb, (b) triangular, (c) random circular, (d) squares, (e-g) 3D models used for simulation having various internal architectures with variable pore sizes and geometries, and (h) scaffold generated by ntopology software.

We created a bone tissue utilizing an algorithm and computation-based design software called nTopology to simulate the flow. In comparison to the real pore size of bone tissue, the average pore size was  $500 \mu m$  [18]. The scaffold cube's overall dimensions were determined to be  $10 mm \times 10 mm \times 10 mm$  to fit in our perfusion, as shown in Figure 1(h). A 3D printer called the Ender 3 (Creality, Shenzhen, China) was used to print several of the scaffolds in Figure 1(a-d). We utilized Form3+ because the bone scaffold in Figure 1(h) was uneven in shape and tiny in scale (Formlabs, Somerville, MA).

#### 2.3 Flow simulation

All fluid flows were performed using the SOLIDWORKS simulation package at varying intake masses of 0.1g/s, 0.2g/s, 0.5g/s, and 1g/s and environmental pressures of 101325 Pa, 151987 Pa, 202650 Pa, and 253312 Pa. Throughout each simulation run, a temperature of  $20.15^{\circ}$ C was maintained. 4% Alginate(A) and 4% Carboxymethyl Cellulose (CMC, C) and 2% Alginate and 6% CMC were two of our designed biomaterial compositions that were used as scaffold materials in the simulation. They will be referred to as  $A_4C_4$  and  $A_2C_6$ . At a shear rate of  $1.0 \text{ s}^{-1}$ , the viscosities of  $A_4C_4$  and  $A_2C_6$  are 965966 mPa.s. and 534040 mPa.s, respectively. A circular and square bone scaffold was printed. Scaffolds were scaled doubled (38 mm diameter/width and 3 mm thickness) to make the scaffolds printable. The beam diameter used for circular and square scaffolds were 0.5mm and 0.35mm respectively. We will print them with the proper hydrogels in the future to ensure their interior architecture.

#### 3. Results and discussions

## 3.1 Simulation result for the scaffolds having uniform internal pore size and geometries.

To determine how the internal geometry of the scaffold that would house the cells in the bioreactor might impact the flow of the media inside, different configurations of the scaffold were investigated. An internal SolidWorks flow simulation was used for the experiments. A set scaffolds shown in Figure 3 were patterns tested. The feasibility of these scaffolds in actual environments was also tested. As the simulations depict an ideal situation, we could determine whether scaffolds are feasible to produce at this scale by printing the scaffolds at full size, 10mm in diameter.

The simulation results shown in Figure 3 (a-b) show that the honeycomb pattern, like the rhombi, didn't work well. The velocity distribution indicates that it created a great amount turbulence. The 3D printed model also didn't come out as defined due to the scale issue and ended up looking more like circles than hexagons. The triangle pattern performed admirably in the simulations. Although this pattern didn't print effectively, fluid could pass through it without creating any turbulence that could injure the cells. It is evident from the velocity pattern in Figure 3(d) that fluid flows at high velocities into and out of the chamber, but at low velocities within the chamber itself.

The circles arranged in a grid pattern worked comparatively better than when arranged in a hexagonal pattern since fluid seemed to flow through most of the pores in the grid pattern configuration whereas on the hexagonal pattern configuration it seems that the fluid wasn't flowing through the pores as evenly. The grid pattern had a similar result to the squares when printed, but the hexagonal pattern didn't print well at all. Both scenarios are shown in Figure 4. The square pattern worked the best in all categories. It prints well, allows fluid to pass through, and doesn't cause additional turbulence and has been the pattern we have been using in the reactor.

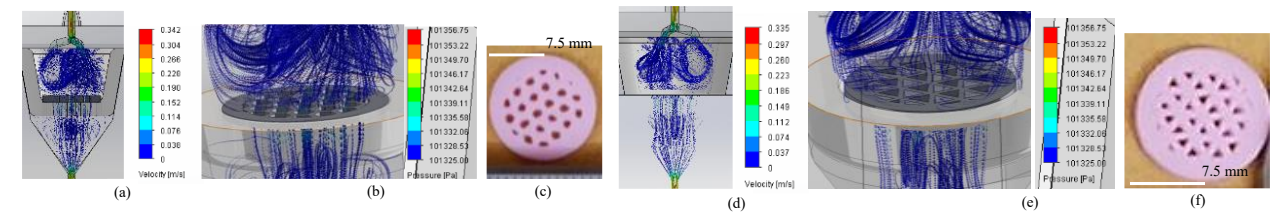


Figure 3: Velocity distribution into the bioreactor chamber while incubated scaffold having (a) honeycomb pattern pores, (d) triangular pattern; turbulence created by the scaffold having (b) honeycomb pattern pores, (e) triangular pores; 3D printed parts of the (c) Honeycomb mode, and (f) Triangular model.

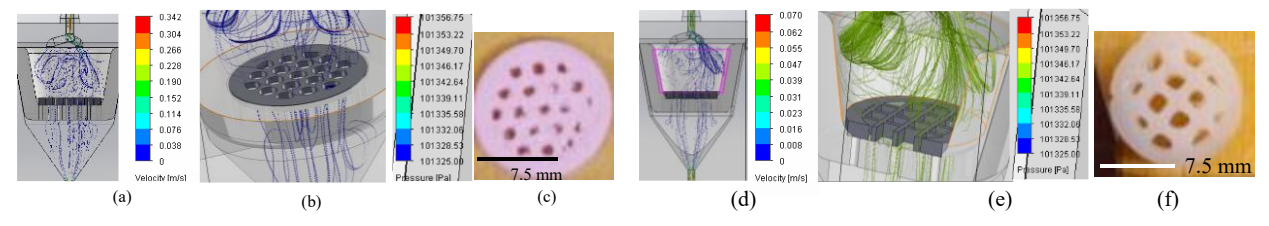


Figure 4: Velocity distribution into the bioreactor chamber while incubated scaffold having (a) random circular array, (d) square patterns; turbulence created by the scaffold having (b) random circular array, (e) square patterns; 3D printed parts of the (c) random circular array, and (f) square patterns.

## 3.2 Simulation result for the scaffolds having variational internal pore size and geometries.

Like the earlier simulations, we performed simulations to verify the interior geometry of the scaffolds having variational porosity. These scaffolds had pores of varied sizes to imitate biological tissue more closely, such as bone tissue, where pores are not uniform in size and are not neatly aligned. Since they performed best in the previous simulations, circles and squares were chosen for these simulations. However, since the medium is intended to contact the scaffold as it flows through to nourish the cells and remove waste, if the pores are too big, the medium was observed to pass through without touching the scaffold, which defeats its purpose. This is true for both the arrangements with square/rectangular pores as shown in Figures 5(a-d). At the beginning, one structure with circular pores that varied in size was modeled (Figure 5(a-b)). We modeled the other as illustrated in Figure 5(c) to address the first's high exposed surface areas, which increased turbulence in the perfusion chamber 5(c-d).

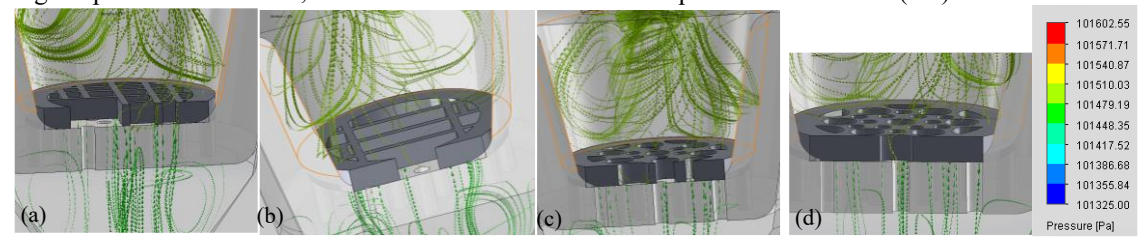


Figure 5: Velocity distribution into the bioreactor chamber while incubated scaffold having various pore sizes and geometries.

We determined the interior shape of our scaffolds using the output from both sets of simulations. As they can be evenly dispersed with a consistent amount of surface area between them, tessellate shapes are the best, and this was our initial conclusion. This can limit the amount of turbulence. According to the second, the pores need to be 1.50mm-2.0mm wide so that the medium may pass through and contact the scaffold, and they need to be 0.50mm-0.75mm apart to prevent leaving a lot of exposed surface area for the medium to bounce off. Based on this information, we chose squares for the internal geometry of the scaffolds since they satisfy all our requirements.

#### 3.3 Simulation result for smaller pore size

We tested the fluid flow through smaller square pores after determining that squares work best for pore shape in 3D printed scaffolds to investigate if the increased amount of exposed surface area would cause unfavorable turbulence in the perfusion chamber as demonstrated in simulations with different shapes. The pores were squares of 0.5 mm by 0.5 mm, spaced 0.5 mm apart, and had flow masses of 0.1, 0.2, and 1.0 g/s. The velocity distribution for the mass flows of 0.1, 0.2, 0.5, and 1.0 g/s shows unequivocally that turbulence will increase as mass flow increases. The rate

of fluid flow through the chamber's entrance and exit points shows a tendency for turbulence to decrease as flow mass increases. As a result, as shown in Figure 6, it was exhibiting an 877% higher velocity (0.596mm/s) for a flow mass of 1.0 g/s than for a flow mass of 0.1 g/s (0.061mm/s).

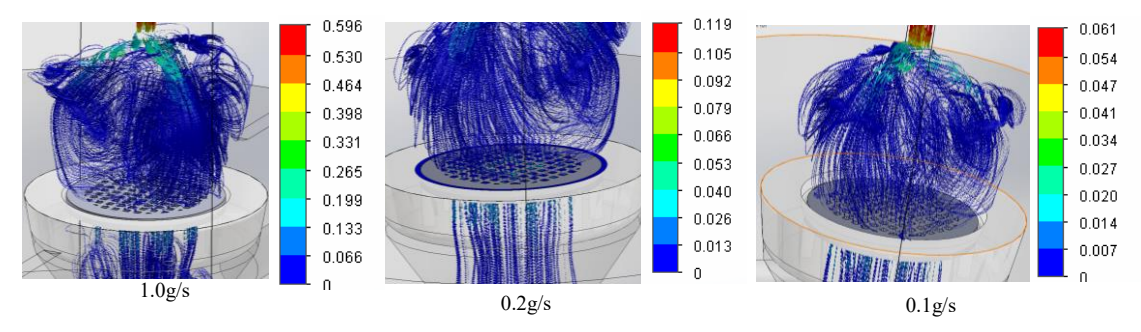


Figure 6: 3D model with smaller pore sizes used for simulation having various mass flow such as 0.1g/s, 0.2g/s, 0.5g/s, and 1.0g/s

## 3.4 Fluid flow through bone tissue prototype

To mimic the bone scaffold, we designed shown in sectional view, a computer with more processing power was needed. As a result, we printed the models to carry out an actual experiment. A model of the circular bone scaffold illustrated in Figure 7 (a) was manufactured to determine the capacity of fluid flow through the bone tissue we constructed in section 2.2. Figure 6(b) illustrates how microscopic examination of the lattice of circular and square scaffolds indicated that thinner beams might produce better interior architecture. Because we observed cleaner lattice structure for square (beam diameter: 0.35 mm) scaffold than circular (beam diameter: 0.50 mm) scaffold. We took a part (10 mm) of the scaffolds and incubated them in our designed and manufactured perfusion bioreactor to make the scaffolds fit in our manufactured bioreactor. Two distinct flow rates, such as 10 ml/s and 2 ml/s, were used for the 20-minute flow of fluid. As depicted in Figure 7 (c), we saw that fluid passed through each scaffold at both flow rates without any overflow. In the future, we'll use enough computing power to run the simulation test.

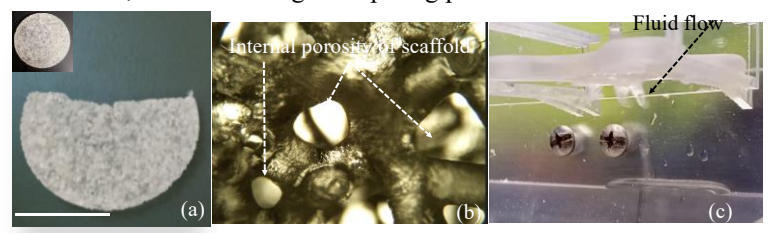


Figure 7: (a) 3D printed scaffolds with resin 3d printer, (b) internal porosity of the printed scaffold, (c) fluid flow through the scaffold.

## 4. Conclusion

In this study, we present a simulation technique where the internal geometries of the scaffolds can be determined from the simulation test results. By changing the process parameters of any perfusion bioreactor, this technique can be applied to other bioreactor chambers. The outcome of our first test led us to the conclusion that tessellate forms are the best since they can be evenly distributed and have a fixed surface area between them, which can manage the amount of turbulence. Also, we discovered that the pores must be  $1500-2000~\mu m$  wide for the medium to pass through. There should be  $500-750~\mu m$  between each pore to ensure that fluid flow makes touch with the scaffold. In future, we will compare the actual fluid flow results with simulated test results. Afterward, we will move on to use our bioreactor to culture cells in the scaffolds. This will allow us to study the functionality of our scaffold designs, and lead to more research towards the development of creating viable three-dimensional scaffolds.

## Acknowledgements

Research was supported by New Hampshire-EPSCoR through BioMade Award #1757371 from National Science Foundation and New Hampshire-INBRE through an Institutional Development Award (IDeA), P20GM103506, from the National Institute of General Medical Sciences of the NIH.

#### References

- [1] S. V. Murphy and A. Atala, "3D bioprinting of tissues and organs," *Nature biotechnology*, vol. 32, no. 8, pp. 773-785, 2014.
- [2] H.-J. Kong, K. Y. Lee, and D. J. Mooney, "Decoupling the dependence of rheological/mechanical properties of hydrogels from solids concentration," *Polymer*, vol. 43, no. 23, pp. 6239-6246, 2002.
- [3] J. Malda *et al.*, "25th anniversary article: engineering hydrogels for biofabrication," *Advanced materials*, vol. 25, no. 36, pp. 5011-5028, 2013.
- [4] C. Mandrycky, Z. Wang, K. Kim, and D.-H. Kim, "3D bioprinting for engineering complex tissues," *Biotechnology Advances*, vol. 34, no. 4, pp. 422-434, 2016/07/01/ 2016, doi: https://doi.org/10.1016/j.biotechadv.2015.12.011.
- [5] P. Lewis and R. N. Shah, "3D-Printed gelatin scaffolds of differing pore size and geometry modulate hepatocyte function and gene hxpression," (in English), *Frontiers in Bioengineering and Biotechnology*, Abstract, doi: 10.3389/conf.FBIOE.2016.01.01756.
- [6] S. M. Mueller, S. Mizuno, L. C. Gerstenfeld, and J. Glowacki, "Medium Perfusion Enhances Osteogenesis by Murine Osteosarcoma Cells in Three-Dimensional Collagen Sponges," *Journal of Bone and Mineral Research*, vol. 14, no. 12, pp. 2118-2126, 1999.
- [7] G. N. Bancroft, V. I. Sikavitsas, and A. G. Mikos, "Technical note: Design of a flow perfusion bioreactor system for bone tissue-engineering applications," *Tissue engineering*, vol. 9, no. 3, pp. 549-554, 2003.
- [8] F. W. Janssen, J. Oostra, A. van Oorschot, and C. A. van Blitterswijk, "A perfusion bioreactor system capable of producing clinically relevant volumes of tissue-engineered bone: in vivo bone formation showing proof of concept," *Biomaterials*, vol. 27, no. 3, pp. 315-323, 2006.
- [9] M. Bartnikowski, T. J. Klein, F. P. Melchels, and M. A. Woodruff, "Effects of scaffold architecture on mechanical characteristics and osteoblast response to static and perfusion bioreactor cultures," *Biotechnology and bioengineering*, vol. 111, no. 7, pp. 1440-1451, 2014.
- [10] V. Mironov, V. Kasyanov, and R. R. Markwald, "Organ printing: from bioprinter to organ biofabrication line," *Current opinion in biotechnology*, vol. 22, no. 5, pp. 667-673, 2011.
- [11] V. Mironov, V. Kasyanov, C. Drake, and R. R. Markwald, "Organ printing: promises and challenges," *Regenerative medicine*, vol. 3, no. 1, pp. 93-103, 2008.
- [12] V. Mironov, R. P. Visconti, V. Kasyanov, G. Forgacs, C. J. Drake, and R. R. Markwald, "Organ printing: tissue spheroids as building blocks," *Biomaterials*, vol. 30, no. 12, pp. 2164-2174, 2009.
- [13] S. P. Hoerstrup, R. Sodian, J. S. Sperling, J. P. Vacanti, and J. E. Mayer Jr, "New pulsatile bioreactor for in vitro formation of tissue engineered heart valves," *Tissue engineering*, vol. 6, no. 1, pp. 75-79, 2000.
- [14] K. Dumont *et al.*, "Design of a new pulsatile bioreactor for tissue engineered aortic heart valve formation," *Artificial organs*, vol. 26, no. 8, pp. 710-714, 2002.
- [15] D. W. Hutmacher and H. Singh, "Computational fluid dynamics for improved bioreactor design and 3D culture," *Trends in biotechnology*, vol. 26, no. 4, pp. 166-172, 2008.
- [16] M. S. Hossain, D. Bergstrom, and X. Chen, "Modelling and simulation of the chondrocyte cell growth, glucose consumption and lactate production within a porous tissue scaffold inside a perfusion bioreactor," *Biotechnology Reports*, vol. 5, pp. 55-62, 2015.
- [17] L. A. Hidalgo-Bastida, S. Thirunavukkarasu, S. Griffiths, S. H. Cartmell, and S. Naire, "Modeling and design of optimal flow perfusion bioreactors for tissue engineering applications," *Biotechnology and Bioengineering*, vol. 109, no. 4, pp. 1095-1099, 2012.
- [18] O. Ball, B.-N. B. Nguyen, J. K. Placone, and J. P. Fisher, "3D printed vascular networks enhance viability in high-volume perfusion bioreactor," *Annals of biomedical engineering*, vol. 44, no. 12, pp. 3435-3445, 2016.
- [19] A. Abbatiello and M. A. Habib, "Development of an In-House Customized Perfusion-Based Bioreactor for 3D Cell Culture," in *International Manufacturing Science and Engineering Conference*, 2022, vol. 85802: American Society of Mechanical Engineers, p. V001T01A016.